Spectrum and Energy Efficiency Tradeoff in IRS-Assisted CRNs with NOMA: A Multi-Objective Optimization Framework

Yuhang Wu, Fuhui Zhou, *Senior Member, IEEE*, Wei Wu, Qihui Wu, *Senior Member, IEEE*,
Rose Qingyang Hu, *Fellow, IEEE*, Kai Kit Wong, *Fellow, IEEE*
Email: *wuyuhang.nuaa@gmail.com, zhoufuhui@ieee.org, wuqihui2014@sina.com, weiwu@njupt.edu.cn, rose.hu@usu.edu, kaikit.wong@ucl.ac.uk*

***Abstract*—Non-orthogonal multiple access (NOMA) is a promising candidate for the sixth generation wireless communication networks due to its high spectrum efficiency (SE), energy efficiency (EE), and better connectivity. It can be applied in cognitive radio networks (CRNs) to further improve SE and user connectivity. However, the interference caused by spectrum sharing and the utilization of non-orthogonal resources can downgrade the achievable performance. In order to tackle this issue, intelligent reflecting surface (IRS) is exploited in a downlink multiple-input-single-output (MISO) CRN with NOMA. To realize a desirable tradeoff between SE and EE, a multi-objective optimization (MOO) framework is formulated. An iterative block coordinate descent (BCD)-based algorithm is exploited to optimize the beamforming design and IRS reflection coefficients iteratively. Simulation results demonstrate that the proposed scheme can achieve a better balance between SE and EE than baseline schemes.**

***Index Terms*—Intelligent reflecting surface, cognitive radio, non-orthogonal multiple access, spectral efficiency, energy efficiency, multi-objective optimization, block coordinate descent.**

I. Introduction

THE fifth generation (5G) wireless communication networks have been commercially deployed and their footprint will be continuously expanded worldwide. Although they have made great breakthrough advancements in wireless communication techniques, performance limitations have gradually appeared along with the unprecedented proliferation of user connectivity, the emergence of diverse real-time and ultra-wideband communication services, and the urgent requirement of green operations [1], [2]. The research initiatives towards sixth generation (6G) wireless communication networks aim to address these performance limitations since their inception. Non-orthogonal multiple access (NOMA) has been envisioned as a candidate multiple access scheme for the 6G wireless communication networks since it can improve both spectrum efficiency (SE) and energy efficiency (EE), and increase user connectivity [3].

The application of NOMA into cognitive radio networks (CRNs) can further boost both SE and EE, and enhance user connectivity [4]. Recently, many researchers have focused on the resource allocations in CRNs with NOMA [4]-[7]. The authors in [5] studied a full-duplex CRNs with NOMA, where an iterative algorithm was proposed to maximizing the throughput of the secondary networks. The results showed that the achievable throughput of CRNs with NOMA is superior to that of CRNs with OMA. The authors in [6] proposed an efficient algorithm in CRNs with NOMA by using the sequential convex approximation method to enhance EE. In [7], the minimization of the transmit power was investigated in MISO CRNs with NOMA relying on simultaneous wireless information and power transfer (SWIPT) under a practical non-linear EH model.

Although NOMA can further improve the SE and user connectivity of CRNs, the complexity of the receiver and interference caused by using non-orthognal resource increase with the number of NOMA users, which results in unpractical design and even poor performance. Recently, intelligent reflecting surface (IRS) has been identified as revolutionary technology due to its potential of simultaneously improving EE and SE [8]. Specifically, IRS can intelligently regulate the phase shifts of its reflecting elements to improve the desired signal power and mitigate the interference at the same time, thereby improving system SE without further energy consumption [9]. Hence, the IRS technique has been exploited in the system with NOMA to tackle the inherent disadvantages of NOMA [11]-[13]. In [11], the ideal and non-ideal IRS assumptions were considered in the sum rate maximization by jointly optimizing the active and passive beamforming vectors subject to SIC decoding rate conditions and IRS reflection coefficients constraints. A novel SIC decoding order searching algorithm was proposed in the IRS-assisted system with NOMA via maximizing the combined channel power gains of each user in [12]. The joint power allocation and phase shift optimization problems were tackled by using the alternative optimization (AO) algorithm and semidefinite relaxation (SDR) method. In contrast to the work in [11] and [12], the work in [13] focused on the energy-efficient design of IRS-assisted systems with NOMA, in which the system EE was maximized by alternatively optimizing the transmit beamforming and the IRS reflection coefficients. The work in [11]-[13] illustrated that the employment of IRS is of immense benefit to the system with NOMA.

Although resource allocation problems have been well studied in CRNs with NOMA [4]-[7] and IRS-assisted NOMA systems [11]-[13], to the best authors' knowledge, there are no investigations focused on resource allocation schemes in the IRS-assisted CRNs with NOMA. Moreover, the resource allocation schemes for IRS-assisted CRNs with OMA proposed in [14] are inappropriate to IRS-assisted CRNs with NOMA since the non-orthogonal resources are utilized. Thus, in order to further improve both SE and EE and provide massive connectivity, it is of great importance to study the resource allocation problems in IRS-assisted MISO CRNs with NOMA.

In this paper, a multi-objective optimization (MOO) framework is formulated in IRS-assisted downlink MISO CRNs with NOMA to simultaneously optimize SE and EE while addressing the tradeoff between them. The formulated problem is nonconvex and intractable. The ϵ-constraint method is adopted to transform the MOO problem (MOOP) into single-objective optimization problem (SOOP). Moreover, a block coordinate descent (BCD)-based iterative algorithm is proposed, where the original problem is decomposed into two sub-optimization problems to design the optimal beamforming vectors and the phase shift iteratively. Simulation results demonstrate that the exploitation of IRS in CRNs with NOMA can achieve a better balance between SE and EE. Moreover, it is shown that our proposed resource allocation schemes can simultaneously improve EE and SE compared to the benchmark schemes.

II. System Model

A. System Model

An IRS-assisted downlink CRN with NOMA is considered, which consists of a licensed primary network and an unlicensed secondary network. Specifically, the primary network comprises one primary base station (PBS) and K PUs, while the secondary network contains one secondary base station (SBS) and N SUs. Let $\mathcal{K} = \{1, 2, \ldots, K\}$ and $\mathcal{N} = \{1, 2, \ldots, N\}$ denote the set of PUs and SUs, respectively. The SBS is equipped with N_s antennas, while the PBS, K PUs and N SUs are all equipped with a single antenna. Besides, an IRS with M passive reflecting elements, denoted by $\mathcal{M} = \{1, 2, \ldots, M\}$, is deployed in the secondary network to enhance the transmission from the SBS to SUs. The diagonal phase shift matrix of IRS is denoted by $\mathbf{\Theta} = \mathrm{diag}\{\beta_1 e^{j\theta_1}, \beta_2 e^{j\theta_2}, \ldots, \beta_M e^{j\theta_M}\}$, where $\beta_m \in [0, 1]$ and $\theta_m \in [0, 2\pi]$ denote the amplitude and phase shift of the mth passive reflecting elements, respectively.

In order to realize NOMA, the superposition coding is employed at the SBS. The data flow for each SU is assigned with a dedicated beamforming vector. Thus, the transmitted superposition of K data flows from the SBS to the SUs can be given as $\boldsymbol{x} = \sum_{n=1}^{N} \mathbf{w}_n x_n$, where $x_n \sim \mathcal{CN}(0, 1)$ and $\mathbf{w}_n \in \mathbb{C}^{N_s \times 1}$ are the data flow intended to the nth SU and the corresponding beamforming vector, respectively.

Let $\mathbf{h}_{k,I} \in \mathbb{C}^{N_s \times 1}$ and $\mathbf{f}_{k,R} \in \mathbb{C}^{M \times 1}$ denote the channel vector between the SBS and the kth PU and the channel vector between the IRS and the kth PU, respectively. The channel between the SBS and the nth SU is denoted by $\mathbf{g}_{n,D} \in \mathbb{C}^{N_s \times 1}$. $\mathbf{g}_{n,R} \in \mathbb{C}^{M \times 1}$ denotes the reflecting channel between the IRS and the nth SU. The channel between the PBS and the nth SU is denoted by $f_{n,D}^{P}$. The baseband equivalent channel between the SBS and the IRS and the channel between the PBS and the IRS are modeled as $\mathbf{g}_{SI} \in \mathbb{C}^{M \times N_s}$ and $\mathbf{f}_{PI} \in \mathbb{C}^{M \times 1}$, respectively. The transmit power from the PBS to the kth PU is denoted by $p_k^P \in \mathbb{R}$, and the information symbol for the kth PU transmitted by PBS is represented by $s_k \in \mathbb{C}$. $n_k \sim \mathcal{CN}(0, \sigma^2)$ and $n_n \sim \mathcal{CN}(0, \sigma^2)$ are the additive white Gaussian noises (AWGNs) at the kth PU and the nth SU, respectively.

According to the NOMA principle, SIC is employed at the SUs to remove the co-channel interference. An optimal SIC decoding order plays a vital role in systems with NOMA, which is determined by the channel power gains. However, in IRS-assisted CRNs with NOMA, the combined channel power gains are influenced by changing the phase shift matrix of IRS, i.e., $\mathbf{\Theta}$. Thus, the low-complexity decoding order search algorithm proposed in [12] is first adopted to obtain the SIC decoding order. Let n represents that the signal of nth SU is the nth signal to be decoded, while the signal of the ith SU with $i > n$ is treated as interference. The signal of the mth SU with $m < n$ is previously decoded at the nth SU and is removed from the received signal. Thus, the achievable signal-to-interference-plus-noise ratio (SINR) at the nth SU to decode its own signal can be written as $\mathrm{SINR}_{n\to n} = \frac{\left|(\boldsymbol{g}_{n,D}^H + \boldsymbol{g}_{n,R}^H \mathbf{\Theta} \boldsymbol{g}_{SI})\mathbf{w}_n\right|^2}{\sum_{i>n}^{N} \left|(\boldsymbol{g}_{n,D}^H + \boldsymbol{g}_{n,R}^H \mathbf{\Theta} \boldsymbol{g}_{SI})\mathbf{w}_i\right|^2 + \sum_{k=1}^{K} \left|f_{n,D}^P + \boldsymbol{g}_{n,R}^H \mathbf{\Theta} \boldsymbol{f}_{PI}\right|^2 p_k^P + n_n}$. The corresponding achievable rate at the nth SU to decode its own signal is represented as $R_{n\to n} = \log_2(1 + \mathrm{SINR}_{n\to n})$. Moreover, the jth SU with $j > n$ is able to decode the signal of the nth SU. The corresponding SINR for the jth SU decoding the signal intended to the nth SU can be expressed as $\mathrm{SINR}_{n\to j} = \frac{\left|(\mathbf{g}_{j,D}^H + \mathbf{g}_{j,R}^H \mathbf{\Theta} \mathbf{g}_{SI})\mathbf{w}_n\right|^2}{\sum_{i>n}^{N} \left|(\boldsymbol{g}_{j,D}^H + \boldsymbol{g}_{j,R}^H \mathbf{\Theta} \mathbf{g}_{SI})\mathbf{w}_i\right|^2 + \sum_{k=1}^{K} \left|f_{j,D}^P + \mathbf{g}_{j,R}^H \mathbf{\Theta} \mathbf{f}_{PI}\right|^2 p_k^P + n_j}$. Hence, the achievable rate of the jth SU to decode the signal of the kth SU is $R_{n\to j} = \log_2(1 + \mathrm{SINR}_{n\to j})$.

Moreover, the power allocated to each SU should be inversely proportional to its channel strength based on the given decoding orders, which can avoid the case that the high decoding order SU uses most of the wireless resources [12]. Therefore, the following condition should be satisfied

$$\left|(\mathbf{g}_{n,D}^H + \mathbf{g}_{n,R}^H \mathbf{\Theta} \mathbf{g}_{SI})\mathbf{w}_i\right|^2 \le \left|(\mathbf{g}_{n,D}^H + \mathbf{g}_{n,R}^H \mathbf{\Theta} \mathbf{g}_{SI})\mathbf{w}_j\right|^2, \quad \forall n \in \mathcal{N}, i, j \in \mathcal{N}, i > j. \tag{1}$$

The inequalities in (5) ensures the successful SIC implemented at the stronger SU and achieve fairness among SUs.

To protect the QoS of the PU, the interference power constraint needs to be considered, given as

$$\sum_{n=1}^{N} \left|(\mathbf{h}_{k,I}^H + \mathbf{f}_{k,R}^H \mathbf{\Theta} \mathbf{g}_{SI})\mathbf{w}_n\right|^2 \le p_{tol,k}, \forall k, \tag{2}$$

where the maximum interference that the kth PU can tolerate is denoted by $p_{tol,k}$.

The total system energy consumption consists of the transmit power and the circuit power consumption. The circuit power consumption denoted by P_c, which is from the circuit power consumed by the SBS, i.e., $P_c = P_{SBS}$, where P_{SBS} denote the power consumption of the SBS. In order to protect the transmitter, the maximum power constraint needs to be satisfied, which is given as

$$P_{tot} = \sum_{n=1}^{N} ||\mathbf{w}_n||^2 + P_c \leq P_{\max}. \tag{3}$$

B. Problem Formulation

In order to comprehensively investigate the tradeoff between EE and SE in the downlink IRS-assisted CRN with NOMA, an MOOP framework is adopted to simultaneously optimize those two objectives. EE is defined as the ratio of the system transmission rate to the total power consumption, while SE is defined as the ratio of the system throughput to the total transmission bandwidth. Accordingly, the EE and SE can be respectively expressed as $\eta_{EE} = \frac{\sum_{n=1}^{N} R_{n\to n}}{P_{tot}}$, $\eta_{SE} = \sum_{n=1}^{N} R_{n\to n}$. Then, the MOOP is formulated as

$$\begin{aligned}
\mathbf{P}_1 : &\max_{\mathbf{w},\mathbf{\Theta}} \ \eta_{SE}, && \text{(4a)}\\
&\max_{\mathbf{w},\mathbf{\Theta}} \ \eta_{EE}, && \text{(4b)}\\
\text{s.t. } & C1 : R_{n\to n} \geq R_{\min}, n \in \mathcal{N} && \text{(4c)}\\
& C2 : |[\mathbf{\Theta}]_{mm}| \leq 1, \forall m, && \text{(4d)}\\
& (1) - (3), && \text{(4e)}
\end{aligned}$$

where i, j, and n denote the decoding index of the ith SU, the jth SU and the nth SU, respectively. The constraint $C1$ indicates the minimum quality of service (QoS) requirement of each SU, where $R_{\min}$ is the minimum rate requirement. The constraint $C2$ is the reflection coefficients constraint. The constraint (1) is served as the SIC constraint which facilitates the successful SIC implementation at SUs. The constraint (2) guarantees that the maximum interference leakage at the kth PU is tolerable.

It is evident that problem $\mathbf{P}_1$ is a challenging non-convex MOOP. The objective function (4b) is a fractional function, and the beamforming vector and IRS phase shift matrix are highly coupled. In order to tackle the highly-coupled non-convex MOOP, we transform problem $\mathbf{P}_1$ into a SOOP and then decompose the original problem into two subproblems of beamforming optimization and reflection coefficients optimization. An alternative algorithm is proposed to tackle this challenging problem.

III. Joint Beamforming and Phase Shift Optimization

A. Problem Reformulation

To tackle the MOOP, the ϵ-constraint method is employed [16]. In particular, the EE maximization is kept as the objective function and the objective function of SE maximization is transformed into a constraint. Thus, the corresponding SOOP can be given as

$$\begin{aligned}
\mathbf{P}_2 : &\max_{\mathbf{w},\mathbf{\Theta}} \eta_{EE}, && \text{(5a)}\\
&\text{s.t. } \eta_{SE} \geq \epsilon, && \text{(5b)}\\
&\text{(4c)-(4e)}, && \text{(5c)}
\end{aligned}$$

where constraint (12b) guarantees the sum throughput of the secondary network is larger than ϵ.

Remark 1: The feasibility of $\mathbf{P}_4$ is significantly dependent on the value of ϵ. Note that the value of ϵ should not be larger than the maximum η_{SE} [16]. Thus, the ϵ can be specified as a value in $(0, \eta_{SE,\max}]$ after solely maximizing η_{SE}.

Due to the highly coupled variables and the fractional form of the objective function, the problem $\mathbf{P}_4$ is still non-convex and intractable. In order to solve this problem, a BCD-based iterative algorithm is proposed. The beamforming vectors are first optimized with the given phase shift matrix, then the phase shift matrix design is optimized with the obtained feasible beamforming vectors.

B. Beamforming Design for Given IRS Phase Shift

Let $\mathbf{W}_n = \mathbf{w}_n\mathbf{w}_n^H$, $\mathbf{W}_n \in \mathbb{H}^{N_s}$. Then, the active beamforming optimization can be rewritten as

$$\begin{aligned}
\mathbf{P}_{2.1} : &\max_{\mathbf{W}_n} \frac{\sum\limits_{n=1}^{N} R_{n\to n}}{\sum\limits_{n=1}^{N} \text{Tr}\left(\mathbf{W}_n\right) + p_c}, && \text{(6a)}\\
&\text{s.t. } C1, (5b), && \text{(6b)}\\
&\sum_{n=1}^{N} \text{Tr}\left(\mathbf{W}_n\right) + p_c \leq P_{\max}, && \text{(6c)}\\
&\sum_{n=1}^{N} \text{Tr}\left(\mathbf{W}_n \mathbf{H}_k^H \mathbf{e}\mathbf{e}^H \mathbf{H}_k\right) \leq p_{tol,k}, \forall k, && \text{(6d)}\\
&\text{Tr}(\mathbf{W}_i \mathbf{v}_n^H \mathbf{e}\mathbf{e}^H \mathbf{v}_n) \leq \text{Tr}(\mathbf{W}_j \mathbf{v}_n^H \mathbf{e}\mathbf{e}^H \mathbf{v}_n),\\
&\qquad\qquad i > j, \forall n, i, j \in \mathcal{N}, && \text{(6e)}\\
&\mathbf{W}_n \succeq 0, \forall n, && \text{(6f)}\\
&\text{Rank}\left(\mathbf{W}_n\right) = 1, \forall n. && \text{(6g)}
\end{aligned}$$

where $\mathbf{e} = [\beta_1 e^{j\theta_1}, \beta_2 e^{j\theta_2}, \ldots, \beta_M e^{j\theta_M} \quad 1]^H$, $\mathbf{v}_n = \begin{bmatrix} \text{diag}(\mathbf{g}_{n,R}^H)\mathbf{g}_{SI} \\ \mathbf{g}_{n,D}^H \end{bmatrix}$, $\mathbf{f}_n = \text{diag}(\mathbf{g}_{n,R}^H)\mathbf{f}_{SI}$, $\vartheta_n = f_{n,D}^P + \mathbf{e}^H\mathbf{f}_n$ and $\mathbf{H}_k = \begin{bmatrix} \text{diag}(\mathbf{f}_{k,R}^H)\mathbf{g}_{SI} \\ \mathbf{h}_{k,I}^H \end{bmatrix}$, respectively. Note that constraints (6f) and (6g) are imposed to guarantee that $\mathbf{W}_n = \mathbf{w}_n\mathbf{w}_n^H$ holds after optimization. Problem $\mathbf{P}_{2.1}$ is a non-convex problem due to the fractional form of the objective function and the non-convexity of the constraint (6b). To tackle the problem $\mathbf{P}_{2.1}$, we introduce auxiliary variables α and $\boldsymbol{\gamma} = \{\gamma_1, \ldots, \gamma_N\}$. The equivalent problem can be given as

$$\mathbf{P}_{2.2}: \max_{\mathbf{W}_n,\alpha,\boldsymbol{\gamma}} \quad \alpha, \tag{7a}$$

$$\text{s.t. (6b)} - \text{(6g)}, \tag{7b}$$

$$\frac{\sum_{n=1}^{N} \log_2(1+\gamma_n)}{\sum_{n=1}^{N} \mathrm{Tr}(\mathbf{W}_n) + p_c} \geq \alpha, \tag{7c}$$

$$\mathrm{SINR}_{n\to n} \geq \gamma_n, \forall n. \tag{7d}$$

Although the objective function (7a) is linear, the problem $\mathbf{P}_{2.2}$ is still non-convex. The non-convexity originates from the constrains (7c), (7d) and the rank-one constraint (6g). To deal with the non-convex constraint (7c), we first rewrite it as $\sum_{n=1}^{N}\log_2(1+\gamma_n) \geq \alpha\sum_{n=1}^{N}\mathrm{Tr}(\mathbf{W}_n) + \alpha p_c$. The first right hand term $\alpha\sum_{n=1}^{N}\mathrm{Tr}(\mathbf{W}_n)$ is the joint convex function with respect to α and $\mathbf{W}_n$. By performing the first-order Taylor approximation, the lower bound of $f(\alpha,\mathbf{W}_n) \triangleq \alpha\sum_{n=1}^{N}\mathrm{Tr}(\mathbf{W}_n)$ for a given feasible point $(\alpha^l, \mathbf{W}_n^l)$ in the lth iteration of the SCA is expressed as

$$\begin{aligned} f(\alpha,\mathbf{W}_n) \geq\; & f(\alpha^l,\mathbf{W}_n^l) \\ & + \sum_{n\in\mathcal{N}} \mathrm{Tr}\left(\triangledown_{\mathbf{W}_n} f(\alpha^l,\mathbf{W}_n^l)^H(\mathbf{W}_n - \mathbf{W}_n^l)\right) \\ & + \triangledown_{\alpha} f(\alpha^l,\mathbf{W}_n^l)(\alpha-\alpha^l) \triangleq \widehat{f}(\alpha,\mathbf{W}_n). \end{aligned} \tag{8}$$

Then, concerning the constraint (7d), we further introduce a set of auxiliary variables $I_n, \forall n\in\mathcal{N}$ as the interference-plus-noise power of the data transmission of the nth SU. Hence, constraint (7d) can be transformed as

$$\mathrm{Tr}(\mathbf{W}_n\mathbf{v}_n^H\mathbf{e}\mathbf{e}^H\mathbf{v}_n) \geq \gamma_n I_n, \tag{9a}$$

$$\sum\nolimits_{i=n+1}^{N}\mathrm{Tr}(\mathbf{W}_i\mathbf{v}_n^H\mathbf{e}\mathbf{e}^H\mathbf{v}_n) + |\vartheta_n|^2 p_k^P + \sigma^2 \leq I_n. \tag{9b}$$

Similarly, in the lth iteration of the SCA, a lower bound of $\gamma_n I_n$ in constraint (9a) at a given point (γ_n^l, I_n^l) can be constructed as

$$\begin{aligned} \gamma_n I_n \geq\; & \gamma_n^l {I_n}^l + \gamma_n^l(I_n - {I_n}^l) + {I_n}^l(\gamma_n - \gamma_n^l) \\ \triangleq\; & \widehat{f}(\gamma_n I_n). \end{aligned} \tag{10}$$

Then, the original problem $\mathbf{P}_{2.1}$ is approximated as

$$\mathbf{P}_{2.3}: \max_{\mathbf{W}_n,\alpha,\boldsymbol{\gamma},\boldsymbol{I}} \quad \alpha, \tag{11a}$$

$$\text{s.t. (6b)} - \text{(6g)}, \text{(9b)} \tag{11b}$$

$$\sum_{n=1}^{N}\log_2(1+\gamma_n) \geq \widehat{f}(\alpha,\mathbf{W}_n) + \alpha p_c, \tag{11c}$$

$$\mathrm{Tr}(\mathbf{W}_n\mathbf{v}_n^H\mathbf{e}\mathbf{e}^H\mathbf{v}_n) \geq \widehat{f}(\gamma_n I_n), \forall n. \tag{11d}$$

Note that the remaining non-convexity of problem $\mathbf{P}_{2.3}$ is caused by the rank-one constraint (6g). Hence, the SDR method is adopted to relax the rank-one constraint [14]. Finally, the relaxed problem of problem $\mathbf{P}_{2.3}$ is a convex semidefinite program (SDP), which can be optimally solved via standard convex solvers such as CVX [17]. To verify the tightness of SDR, **Theorem 1** is given.

Theorem 1: The optimal solution of problem $\mathbf{P}_{2.3}$ without the rank-one constraint can always satisfy rank$(\mathbf{W}_n) \leq 1, \forall n\in\mathcal{N}$.

Proof: Please refer to Appendix A. ∎

Note that the obtained objective function of problem $\mathbf{P}_{2.3}$ is served as a lower bound of that in the problem $\mathbf{P}_{2.1}$ owing to the replacement of the constraints (11c) and (11d). Let $\mathbf{W}_n^{\ddagger}, \forall n$ denote the optimal solution of problem $\mathbf{P}_{2.3}$. Since $\mathbf{W}_n^{\ddagger} = \mathbf{w}_n^{\ddagger}\mathbf{w}_n^{\ddagger H}$, the optimal beamforming vector $\mathbf{w}_n^{\ddagger}$ can be obtained by utilizing eigenvalue decomposition.

C. Phase Shift Optimization with Given Beamforming Vector

For given $\mathbf{w}_n$, the IRS phase shift optimization problem can be written as

$$\mathbf{P}_{2.4}: \max_{\boldsymbol{\Theta}} \eta_{SE}, \tag{12a}$$

$$\text{s.t. } C1, C2, (1), (2), (5b). \tag{12b}$$

Note that the objective function and constraints are non-convex with respect to $\boldsymbol{\Theta}$. Therefore, the following transformation is performed to make the optimization problem more tractable. Recall $\mathbf{W}_n = \mathbf{w}_n\mathbf{w}_n^H$, $\mathbf{e} = [\beta_1 e^{j\theta_1}, \beta_2 e^{j\theta_2}, \ldots, \beta_M e^{j\theta_M} \quad 1]^T$, $\mathbf{v}_n = \left[\mathrm{diag}(\mathbf{g}_{n,R}^H)\mathbf{g}_{SI} \quad \mathbf{g}_{n,D}^H\right]^H$, $\mathbf{f}_n = \mathrm{diag}(\mathbf{g}_{n,R}^H)\mathbf{f}_{SI}$, and $\mathbf{H}_k = \left[\mathrm{diag}(\mathbf{f}_{k,R}^H)\mathbf{g}_{SI}\mathbf{h}_{k,I}^H\right]^H$. Similar to the method adopted for solving problem $\mathbf{P}_{2.1}$, by applying SDR and introducing auxiliary variables Γ_n and z_n, the problem $\mathbf{P}_{2.4}$ can be transformed into

$$\mathbf{P}_{2.5}: \max_{\mathbf{E},\boldsymbol{\Gamma},\boldsymbol{z}} \frac{1}{P_{tot}}\sum_{n=1}^{N}\log_2(1+\Gamma_n), \tag{13a}$$

$$\text{s.t. } C1, (5b), \tag{13b}$$

$$\sum_{n=1}^{N}\mathrm{Tr}\left(\mathbf{E}\mathbf{H}_k\mathbf{W}_n\mathbf{H}_k^H\right) \leq p_{tol,k}, \forall k, \tag{13c}$$

$$\mathrm{Tr}\left(\mathbf{E}\mathbf{v}_n\mathbf{W}_i\mathbf{v}_n^H\right) \leq \mathrm{Tr}\left(\mathbf{E}\mathbf{v}_n\mathbf{W}_j\mathbf{v}_n^H\right), i>j, \forall n,i,j\in\mathcal{N}, \tag{13d}$$

$$\mathbf{E}(m,m) \leq 1, m\in\mathcal{M}, \mathbf{E}_{M+1} = 1, \tag{13e}$$

$$\mathbf{E} \succeq 0, \tag{13f}$$

$$\mathrm{Tr}\left(\mathbf{E}\mathbf{v}_n\mathbf{W}_n\mathbf{v}_n^H\right) \geq \Gamma_n z_n, \forall n, \tag{13g}$$

$$\sum_{i=n+1}^{N}\mathrm{Tr}(\mathbf{E}\mathbf{v}_n\mathbf{W}_i\mathbf{v}_n^H) + \sum_{k=1}^{K}\mathrm{Tr}(\mathbf{E}\mathbf{F}_n)p_k^P + n_j \leq z_n. \tag{13h}$$

where $\mathbf{E} \triangleq \mathbf{e}\mathbf{e}^H, \mathbf{E}\in\mathbb{C}^{(M+1)\times(M+1)}$. $\mathbf{F}_n$ is defined as $\mathbf{F}_n = \begin{bmatrix} \mathbf{f}_n\mathbf{f}_n^H & f_{n,D}^{*P}\mathbf{f}_n \\ \mathbf{f}_n^H f_{n,D}^P & |f_{n,D}^P|^2 \end{bmatrix}$. Since variables in the right hand term of constraint (13g) is coupled, the SCA is applied to tackle the non-convexity of constraint (13g). Thus, in the lth iteration of the SCA, the lower bound with the first-order Taylor approximation at the given feasible point (Γ_n^l, z_n^l) can

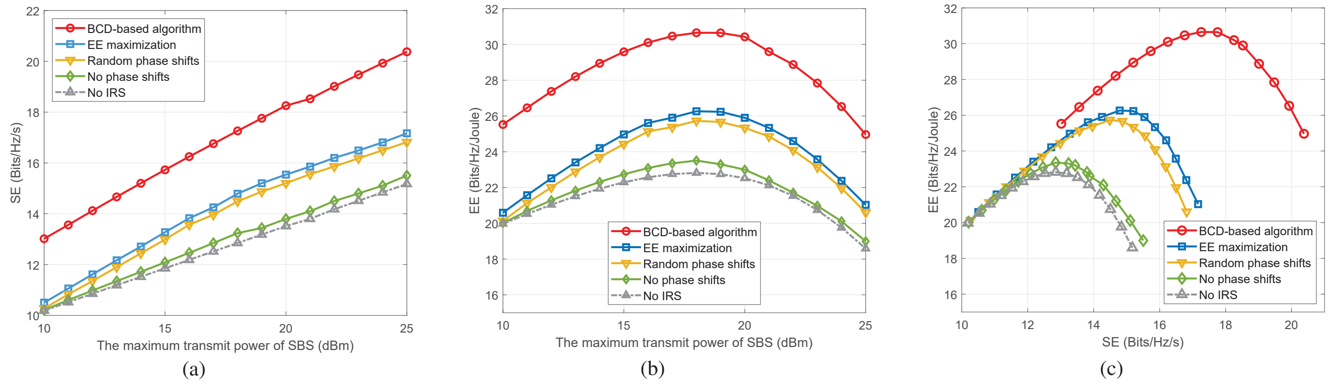

Fig. 1. (a) SE versus the maximum available transmit power; (b) EE versus the maximum available transmit power; (c) EE-SE tradeoff for different schemes.

be given as

$$\Gamma_n z_n \geq \Gamma_n^l {z_n}^l + \Gamma_n^l (z_n - {z_n}^l) + {z_n}^l (\Gamma - \Gamma_n^l) \triangleq \widehat{f}(\Gamma_n z_n). \tag{14}$$

Then, a lower bound of the IRS optimization problem in $\mathbf{P}_{2.5}$ can be obtained by solving the following problem, given as

$$\mathbf{P}_{2.6}: \max_{\mathbf{E},\boldsymbol{\Gamma},\boldsymbol{z}} \frac{1}{P_{tot}} \sum_{n=1}^{N} \log_2 (1 + \Gamma_n), \tag{15a}$$

$$\text{s.t. } (13b) - (13h), \tag{15b}$$

$$\text{Tr}\left(\mathbf{E}\mathbf{v}_n \mathbf{W}_n \mathbf{v}_n^H\right) \geq \widehat{f}(\Gamma_n z_n), \forall n. \tag{15c}$$

The problem $\mathbf{P}_{2.6}$ is a standard SDP problem and the optimal $\mathbf{E}^{\ddagger}$ can be obtained by using the standard convex optimization toolboxes such as CVX [17]. Finally, since $\mathbf{E}^{\ddagger} = \mathbf{e}^{\ddagger}\mathbf{e}^{\ddagger H}$, $\mathbf{e}^{\ddagger}$ can be obtained by eigenvalue decomposition if the rank of $\mathbf{E}^{\ddagger}$ is one. Otherwise, the Gaussian randomization can be adopted to alternatively obtain the approximate $\mathbf{e}$ [14].

IV. Simulation Results

In this section, simulation results are provided to validate the effectiveness of the proposed algorithm. The simulation settings are based on the works in [9]. The locations of the primary and secondary base station are respectively set as $(5, 0, 20)$ and $(5, 100, 20)$. Moreover, the locations of 3 SUs are set as $(5, 165, 0)$, $(5, 145, 0)$ and $(5, 125, 0)$, respectively. The IRS is employed in the secondary network, whose location is set to be $(0, 125, 2)$. The channels are generated by the model $\mathbf{h}_\beta = \sqrt{G_0 (d)^{-c_\beta}} \mathbf{g}_\beta$, where $G_0 = -30$ dB denotes the path loss at the reference point. d denotes the link distance. c_β and $\mathbf{g}_\beta$ denote the path loss exponent and fading component, respectively, where $\beta \in \{D, SI, R\}$. The path loss exponents for the direct link, SBS-IRS link and IRS-user link are set to be $c_D = 3.5$, $c_{SI} = 2.2$ and $c_R = 2.2$, respectively. The bandwidth is normalized as 1 Hz. The minimum rate threshold R_{min} of SUs is set as 0.5 Bits/Hz/s. The interference tolerance of the kth PU is set to be $p_{tol,k} = -90$ dBm. The noise power is set as -110 dBm. The tolerance error of SCA and BCD are set to be $\varepsilon_{SCA} = \varepsilon_{BCD} = 10^-2$.

The proposed algorithm is marked as 'BCD-based algorithm'. For comparison, four baseline schemes are considered. The first baseline scheme aims to maximize EE, which is marked as 'EE maximization'. The second baseline scheme is the method that with the assistance of IRS, the phases of the IRS are generated randomly, denoted by 'Random phase shifts'. For the third baseline scheme, the IRS reflecting coefficients do not have phase adjustment, which is marked by 'No phase shifts'. The fourth baseline scheme is based on the conventional CRN with NOMA without the assistance of IRS, which is marked as 'No IRS'.

Fig. 3(a) and Fig. 3(b) show the SE and EE versus the SBS maximum available transmit power achieved by different designs, respectively. It is seen from Fig. 3(a) that the proposed BCD-based algorithm can achieve the best SE among all schemes. Meanwhile, as shown in Fig. 3(b), the proposed scheme also can achieve a better EE than all baseline schemes. This indicates that the exploitation of IRS in CRNs with NOMA is beneficial for improving both SE and EE. Specifically, in Fig. 3(a), the system SE increases monotonically with the maximum transmit power $P_{\max}$. Moreover, the SE achieved by 'No IRS' baseline scheme is lower than other schemes, which demonstrates that SE can be further improved by the assistance of IRS. As shown in Fig. 3(a), the 'Random phase shifts' and 'No phase shifts' schemes also can achieve better SE performance than those of other baseline scheme without IRS. This indicates that IRS is able to increase the system performance to a certain extent, even without the adjustment of phase shifts.

In order to further illustrate the relationship between SE and EE, Fig. 3(c) shows the tradeoffs between SE and EE of all five schemes in the range of the maximum transmit power constraint from 10dBm to 25 dBm. It is seen that the system EE is a quasi-concave function of SE. When SE increases, EE firstly grows and then decreases with it. It indicates that the achievement of higher SE demands more energy consumption. Meanwhile, EE is the ratio of system throughput to energy consumption. When the energy consumption becomes faster than the growth of SE, EE starts to decrease with the increase of SE. Moreover, the tradeoff achieved by the baseline schemes is presented. It is also seen that the proposed BCD-based algorithm can achieve a better SE-EE tradeoff compared to the other baselines schemes enabled by the joint optimization of SE and EE. It demonstrates that the proposed algorithm has great potential for achieving a superior balance between SE and EE.

V. Conclusion

In this paper, the tradeoff between SE and EE was studied in an IRS-assisted downlink MISO NOMA CRN. The MOOP framework was formulated by simultaneously maximizing SE and EE via jointly optimizing the beamforming design and the reflection coefficients of IRS. The ϵ-constraint method was adopted to transform the MOOP into SOOP. Due to the fact that the variables are highly coupled, a BCD-based algorithm was exploited to optimize the beamforming design and IRS reflection coefficients iteratively. Simulation results demonstrated that the proposed scheme can achieve a better balance between SE and EE than the baseline schemes.

Appendix A
Proof of Theorem 1

The relaxation of problem $\mathbf{P}_{2.3}$ is jointly convex over all optimization variables. Therefore, the optimal solution is characterized by the KKT conditions. In particular, the Lagrangian function of the relaxation of problem $\mathbf{P}_{2.3}$ in terms of the beamforming matrix $\mathbf{W}_n$ can be given as

$$\begin{aligned}\mathcal{L} =& a_1\left(\sum_{n=1}^{N}\log_2\left(1+\gamma_n\right)-\widehat{f}(\alpha,\mathbf{W}_n)\right)\\&+a_2\left(\mathrm{Tr}(\mathbf{W}_n\mathbf{v}_n^H\mathbf{e}\mathbf{e}^H\mathbf{v}_n)-\widehat{f}(\gamma_n I_n)\right)\\&+a_3\left[I_n-\sum_{i=n+1}^{N}\mathrm{Tr}(\mathbf{W}_i\mathbf{v}_n^H\mathbf{e}\mathbf{e}^H\mathbf{v}_n)+|\vartheta_n|^2p_k^P+\sigma^2\right]\\&+a_4\left[P_{\max}-\left(\sum_{n=1}^{N}\mathrm{Tr}\left(\mathbf{W}_n\right)+p_c\right)\right]\\&+a_5\left[p_{tol,k}-\sum_{n=1}^{N}\mathrm{Tr}\left(\mathbf{W}_n\mathbf{H}_k^H\mathbf{e}\mathbf{e}^H\mathbf{H}_k\right)\right]\\&+a_6\left[\mathrm{Tr}\left(\mathbf{W}_j\mathbf{v}_n^H\mathbf{e}\mathbf{e}^H\mathbf{v}_n\right)-\mathrm{Tr}\left(\mathbf{W}_i\mathbf{v}_n^H\mathbf{e}\mathbf{e}^H\mathbf{v}_n\right)\right]\\&+\mathrm{Tr}\left(\mathbf{W}_n\mathbf{Y}_n\right)+\boldsymbol{\Upsilon},\end{aligned}\tag{16}$$

where $\boldsymbol{\Upsilon}$ are the terms independent of $\mathbf{W}_n$, $\boldsymbol{a}$ and $\mathbf{Y}_n$ are Lagrange multipliers associated with the corresponding constraints. By checking the KKT conditions with respect to $\mathbf{W}_n$, for the optimal $\mathbf{W}_n^{\ddagger}$, one has

$$\boldsymbol{a}^{\ddagger}\geq 0,\;\; \mathbf{Y}_n\succeq 0,\;\; \mathbf{Y}_n^{\ddagger}\mathbf{W}_n^{\ddagger}=0,\;\; \bigtriangledown_{\mathbf{W}_n^{\ddagger}}\mathcal{L}=0,\tag{17}$$

where $\boldsymbol{a}^{\ddagger}$ and $\mathbf{Y}_n^{\ddagger}$ are the optimal Lagrange multipliers while the $\bigtriangledown_{\mathbf{W}_n^{\ddagger}}\mathcal{L}$ represents the gradient vector of $\mathcal{L}$ with respect to $\mathbf{W}_n^{\ddagger}$. The $\bigtriangledown_{\mathbf{W}_n^{\ddagger}}\mathcal{L}$ is explicitly expressed as

$$\mathbf{Y}_n^{\ddagger}=a_4\mathbf{I}_{N_s}+\boldsymbol{\Delta}_n^{\ddagger},\tag{18}$$

where $\boldsymbol{\Delta}_n^{\ddagger}$ is given by $a_1\bigtriangledown_{\mathbf{W}_n}\hat{f}(\mathbf{W}_n^{\ddagger})-(a_2+a_6)\,\mathbf{v}_n^H\mathbf{e}\mathbf{e}^H\mathbf{v}_n+a_5\mathbf{H}_k^H\mathbf{e}\mathbf{e}^H\mathbf{H}_k$.

Then, we will prove the optimal beamforming matrix $\mathbf{W}_n^{\ddagger}$ is rank-one by unveiling the structure of matrix $\mathbf{Y}_n^{\ddagger}$. The maximum eigenvalue of matrix $\boldsymbol{\Delta}_n^{\ddagger}$ is denoted by $\nu_{max}\in\mathbb{R}$. Note that due to the randomness of the channels, the probability of the case where multiple eigenvalues have the same value $\nu_{max}\in\mathbb{R}$ is zero. According to (18), if $\nu_{max}>a_4$, $\mathbf{Y}_n^{\ddagger}$ cannot be positive semidefinite which contradicts $\mathbf{Y}_n\succeq 0$. On the other hand, if $\nu_{max}\leq a_4$, $\mathbf{Y}_n^{\ddagger}$ is positive semidefinite with $\mathrm{Rank}(\mathbf{Y}_n^{\ddagger})\geq N_s-1$. According to $\mathbf{Y}_n^{*}\mathbf{W}_n^{\ddagger}=0$, $\mathrm{Rank}(\mathbf{W}_n^{\ddagger})=1$. The proof is completed.

References

[1] S. Dang, O. Amin, B. Shihada, and M.-S. Alouini, "What should 6G be?," *Nat. Electron.*, vol. 3, pp. 20-29, Jan. 2020.

[2] Q. Wu, T. Ruan, F. Zhou, Y. Huang, F. Xu, S. Zhao, Y. Liu, and X. Huang, "A unified cognitive learning framework for adapting to dynamic environment and tasks," *IEEE Wireless Commun.*, to be published, 2021.

[3] L. Dai, B. Wang, Y. Yuan, S. Han, I. Chih-lin and Z. Wang, "Non-orthogonal multiple access for 5G: solutions, challenges, opportunities, and future research trends," *IEEE Commun. Mag.,* vol. 53, no. 9, pp. 74-81, Sep. 2015.

[4] F. Zhou, Y. Wu, Y. Liang, Z. Li, Y. Wang and K. Wong, "State of the art, taxonomy, and open issues on cognitive radio networks with NOMA," *IEEE Wireless Commun.,* vol. 25, no. 2, pp. 100-108, April 2018.

[5] Q. N. Le, A. Yadav, N. -P. Nguyen, O. A. Dobre and R. Zhao, "Full-duplex non-orthogonal multiple access cooperative overlay spectrum-sharing networks with SWIPT," *IEEE Trans. Green Commun. and Netw.,* vol. 5, no. 1, pp. 322-334, Mar. 2021.

[6] Y. Zhang, Q. Yang, T.-X. Zheng, H.-M. Wang, Y. Ju, and Y. Meng, "Energy efficiency optimization in cognitive radio inspired non-orthogonal multiple access," *Proc. IEEE 27th PIMRC,* pp. 1-6, Sep. 2016.

[7] H. Sun, F. Zhou, and Z. Zhang, "Robust beamforming design in a NOMA cognitive radio network relying on SWIPT," *Proc. IEEE Int. Cof. Commun. (ICC),* Kansas City, USA, pp. 1-6, Jul. 2018.

[8] Q. Wu and R. Zhang, "Towards smart and reconfigurable environment: Intelligent reflecting surface aided wireless network," *IEEE Commun. Mag.,* vol. 58, no. 1, pp. 106-112, Jan. 2020.

[9] Q. Wang, F. Zhou, R. Q. Hu, an Y. Qian, "Energy efficient robust beamforming and cooperative jamming design for IRS-assisted MISO networks," *IEEE Trans. Wireless Commun.,* vol. 20, no. 4, pp. 2592-2607, Apr. 2021.

[10] X. Mu, Y. Liu, L. Guo, J. Lin, and N. Al-Dhahir, "Exploiting intelligent reflecting surfaces in NOMA networks: Joint beamforming optimization," *IEEE Trans. Wireless Commun.,* vol. 19, no. 10, pp. 6884-6898, Oct. 2020.

[11] X. Mu, Y. Liu, L. Guo, J. Lin, and N. Al-Dhahir, "Exploiting intelligent reflecting surfaces in NOMA networks: Joint beamforming optimization," *IEEE Trans. Wireless Commun.,* vol. 19, no. 10, pp. 6884-6898, Oct. 2020.

[12] G. Yang, X. Xu, and Y.-C. Liang, "Intelligent reflecting surface assisted non-orthogonal multiple access," *Proc. IEEE Wireless Commun. and Netw. Conf. (WCNC)*, pp. 1-6, May 2020.

[13] F. Fang, Y. Xu, Q.-V. Pham, and Z. Ding, "Energy-efficient design of IRS-NOMA networks," *IEEE Trans. Veh. Tech.,* vol. 69, no. 11, Nov. 2020.

[14] X. Guan, Q. Wu, and R. Zhang, "Joint power control and passive beamforming in IRS-assisted spectrum sharing," *IEEE Commun. Lett.*, vol. 24, no. 7, pp. 1553-1557, Jul. 2020.

[15] J. Tang, D. K. So, E. Alsusa, and K. A. Hamdi, "Resource efficiency: A new paradigm on energy efficiency and spectral efficiency tradeoff," *IEEE Trans. Wireless Commun.,* vol. 13, no. 8, pp. 4656-4669, Aug. 2014.

[16] S. Zarandi, A. Khalili, M. Rasti, and H. Tabassum, "Multi-objective energy efficient resource allocation and user association for in-band full duplex small-cells," *IEEE Trans. Green Commun. and Netw.,* vol. 4, no. 4, pp. 1048-1060, Dec. 2020.

[17] M. Grant and S. Boyd, "CVX: Matlab software for disciplined convex programming, version 2.1," 2014.

[18] S. P. Boyd and L. Vandenberghe, *Convex Optimization.* Cambridge, U.K.: Cambridge Univ. Press, 2004.